

RESEARCH ARTICLE

SSD1 suppresses phenotypes induced by the lack of Elongator-dependent tRNA modifications

Fu Xu , Anders S. Byström *, Marcus J. O. Johansson *

Department of Molecular Biology, Umeå University, Umeå, Sweden

* anders.bystrom@umu.se (ASB); marcus.johansson@umu.se (MJOJ)



 OPEN ACCESS

Citation: Xu F, Byström AS, Johansson MJO (2019) *SSD1* suppresses phenotypes induced by the lack of Elongator-dependent tRNA modifications. PLoS Genet 15(8): e1008117. <https://doi.org/10.1371/journal.pgen.1008117>

Editor: Anita K. Hopper, Ohio State University, UNITED STATES

Received: March 28, 2019

Accepted: August 16, 2019

Published: August 29, 2019

Copyright: © 2019 Xu et al. This is an open access article distributed under the terms of the [Creative Commons Attribution License](https://creativecommons.org/licenses/by/4.0/), which permits unrestricted use, distribution, and reproduction in any medium, provided the original author and source are credited.

Data Availability Statement: All relevant data are within the manuscript and its Supporting Information files.

Funding: This work was supported by Magnus Bergvalls Foundation (2017-02098 to MJOJ); Åke Wibergs Foundation (M14-0207 to MJOJ); Swedish Research Council (621-2016-03949 to ASB); and Karin and Harald Silanders Foundation/Insamlingsstiftelsen Umeå universitet (FS 2.1.6-1870-16 to ASB). The funders had no role in study design, data collection and analysis, decision to publish, or preparation of the manuscript.

Abstract

The Elongator complex promotes formation of 5-methoxycarbonylmethyl (mcm⁵) and 5-carbamoylmethyl (ncm⁵) side-chains on uridines at the wobble position of cytosolic eukaryotic tRNAs. In all eukaryotic organisms tested to date, the inactivation of Elongator not only leads to the lack of mcm⁵/ncm⁵ groups in tRNAs, but also a wide variety of additional phenotypes. Although the phenotypes are most likely caused by a translational defect induced by reduced functionality of the hypomodified tRNAs, the mechanism(s) underlying individual phenotypes are poorly understood. In this study, we show that the genetic background modulates the phenotypes induced by the lack of mcm⁵/ncm⁵ groups in *Saccharomyces cerevisiae*. We show that the stress-induced growth defects of Elongator mutants are stronger in the W303 than in the closely related S288C genetic background and that the phenotypic differences are caused by the known polymorphism at the locus for the mRNA binding protein Ssd1. Moreover, the mutant *ssd1* allele found in W303 cells is required for the reported histone H3 acetylation and telomeric gene silencing defects of Elongator mutants. The difference at the *SSD1* locus also partially explains why the simultaneous lack of mcm⁵ and 2-thio groups at wobble uridines is lethal in the W303 but not in the S288C background. Collectively, our results demonstrate that the *SSD1* locus modulates phenotypes induced by the lack of Elongator-dependent tRNA modifications.

Author summary

Modified nucleosides in the anticodon region of tRNAs are important for the efficiency and fidelity of translation. The Elongator complex promotes formation of several related modified uridine residues at the wobble position of eukaryotic tRNAs. In yeast, plants, worms, mice and humans, mutations in genes for Elongator subunits lead to a wide variety of different phenotypes. Here, we show that the genetic background modulates the phenotypic consequences of the inactivation of budding yeast Elongator. This background effect is largely a consequence of a polymorphism at the *SSD1* locus, encoding a RNA binding protein that influences translation, stability and/or localization of mRNAs. We show that several phenotypes reported for yeast Elongator mutants are either significantly

Competing interests: The authors have declared that no competing interests exist.

stronger or only detectable in strains harboring a mutant *ssd1* allele. Thus, *SSD1* is a suppressor of the phenotypes induced by the hypomodification of tRNAs.

Introduction

A general feature of tRNA molecules is that a subset of their nucleosides harbors post-transcriptional modifications. Modified nucleosides are frequently found in the anticodon region of tRNAs, especially at position 34 (the wobble nucleoside) and 37. Modifications at these positions typically influence the decoding properties of tRNAs by improving or restricting anticodon-codon interactions [1, 2]. Uridines present at the wobble position in eukaryotic cytoplasmic tRNAs often harbor a 5-methoxycarbonylmethyl (mcm^5) or 5-carbamoylmethyl (ncm^5) side-chain and sometimes also a 2-thio (s^2) or 2'-*O*-methyl group [3, 4]. The first step in the synthesis of the mcm^5 and ncm^5 side-chains requires the Elongator complex, which is composed of six Elp proteins (Elp1-Elp6) [5–9]. Elongator is thought to catalyze the addition of a carboxymethyl (cm) group to the 5-position of the uridine which is then converted to mcm^5 by the Trm9/Trm112 complex or to ncm^5 by a yet unidentified mechanism [5, 8–12].

In the budding yeast *Saccharomyces cerevisiae*, the inactivation of any of the six *ELP* genes (*ELP1-ELP6*) not only leads to the lack of the mcm^5/ncm^5 groups but also a slower growth rate and numerous additional phenotypes [5, 13]. These phenotypes include increased sensitivity to elevated temperatures and various chemical stresses as well as defects in transcription, exocytosis, telomeric gene silencing, and protein homeostasis [14–18]. Even though Elongator mutants lack mcm^5/ncm^5 groups in 11 tRNA species [5, 19], the pleiotropic phenotypes are suppressed by increased expression of various combinations of the hypomodified forms of the three tRNA species that normally harbor a $mcm^5s^2U_{34}$ residue, $tRNA_{UUU}^{Lys}$, $tRNA_{UUG}^{Gln}$ and $tRNA_{UUC}^{Glu}$ [18, 20, 21]. These findings suggest the pleiotropic phenotypes of Elongator mutants are caused by a reduced functionality of the hypomodified $tRNA_{UUU}^{Lys}$, $tRNA_{UUG}^{Gln}$ and $tRNA_{UUC}^{Glu}$ in translation [20, 21]. The importance of the modified wobble residue in these tRNAs was supported by the finding that strains lacking the s^2 group show the same but slightly weaker phenotypes that are also suppressed by increased expression of the three tRNAs [20, 21]. Moreover, ribosome profiling experiments have shown that the inactivation of Elongator causes an accumulation of ribosomes with AAA, CAA or GAA codons in the ribosomal A-site [18, 22, 23]. However, the pausing at the codons appears to be relatively small [18, 22] and the mechanism(s) underlying the pleiotropic phenotypes of Elongator mutants are poorly understood.

In yeast, the cell wall stress that arises during normal growth or through environmental challenges is sensed and responded to by the cell wall integrity (CWI) pathway [24, 25]. The CWI pathway is induced by several different types of stresses, including growth at elevated temperatures, hypo-osmotic shock, and exposure to various cell wall stressing agents [25]. A family of cell surface sensors (Wsc1-Wsc3, Mid2 and Mtl1) detects the cell wall stress and recruits the guanine nucleotide exchange factors Rom1 and Rom2 which activate the small GTPase Rho1. Rho1-GTP binds and activates several effectors, including the kinase Pkc1. Pkc1 activates a downstream MAP kinase cascade comprised of the MAPKKK Bck1, the two redundant MAPKK Mkk1 and Mkk2, and the MAPK Mpk1 (Slt2). The phosphorylated Mpk1 then activates factors that promote transcription of genes important for cell wall biosynthesis and remodeling.

In addition to the CWI pathway, several other factors and pathways are known to influence the cell wall remodeling that occurs upon stress, e.g. the mRNA-binding protein Ssd1. Ssd1

has been reported to bind and influence the translation, stability and/or localization of a subset of cellular mRNAs of which many encode proteins important for cell wall biosynthesis and remodeling [26–31]. The wild-type *SSD1* gene was originally identified as a suppressor of the lethality induced by a deletion of the *SIT4* gene, which encodes a phosphatase involved in a wide range of cellular processes [32]. The study also led to the finding that some wild-type *S. cerevisiae* laboratory strains harbor a mutation at the *SSD1* locus that is synthetic lethal with the *sit4Δ* allele [32]. The *SSD1* locus has since been genetically implicated in many cellular processes, including cell wall integrity, various signal transduction pathways, cell morphogenesis, cellular aging, virulence, and transcription by RNA polymerase I, II and III [33–38]. Although the mechanisms by which Ssd1 influences these processes are poorly understood, they possibly involve both direct and indirect effects of Ssd1's influence on messenger ribonucleoprotein (mRNP) complexes [28, 29, 39]. With respect to the transcripts that encode cell wall remodeling factors, Ssd1 seems to act as a translational repressor and this function is controlled by the protein kinase Cbk1, which is a component in the RAM (Regulation of Ace2 and cellular morphogenesis) network [28]. In addition to relieving the translational repression, the phosphorylation of Ssd1 appears to promote polarized localization of some Ssd1-associated mRNAs [28, 31].

In this study, we show that increased activation of the CWI signaling pathway counteracts the temperature sensitive (Ts) growth defect of *elp3Δ* mutants in the W303 but not in the S288C genetic background. Further, the stress-induced growth phenotypes caused by the tRNA modification defect are generally stronger in W303- than in S288C-derived strains. We show that the phenotypic differences are due to the allelic variation at the *SSD1* locus, i.e. the phenotypes are aggravated by the nonsense *ssd1-d2* allele found in the W303 background. We also show that the phenotypes linking the tRNA modification defect to histone acetylation and telomeric gene silencing are caused by a synergistic interaction with the *ssd1-d2* allele. The difference at the *SSD1* locus also provides a partial explanation to the finding [18, 40, 41] that cells lacking both the *mcm⁵* and *s²* group are viable in the S288C but not in the W303 background.

Results

The Ts phenotype of W303-derived *elp3Δ* cells is partially suppressed by increased expression of factors in the CWI signaling pathway

The observation that Elongator mutants are sensitive to cell wall stressing agents, e.g. calcofluor white and caffeine, implies a defect in cell wall integrity [14]. This notion is further supported by the finding that the Ts growth defect of Elongator-deficient cells is partially suppressed by osmotic support (1 M sorbitol) [42]. As the caffeine sensitivity and Ts growth defect are suppressed by increased levels of the hypomodified tRNA^{Lys}_{UUU} and tRNA^{Gln}_{UUG} [20], the phenotypes are likely caused by reduced functionality of these tRNAs in translation. To further define the wall integrity defect in Elongator mutants, we investigated, in the W303 genetic background, if the Ts phenotype of *elp3Δ* cells is suppressed by increased expression of factors in the CWI signaling pathway. The analyses revealed that the introduction of a high-copy *MID2*, *WSC2*, *ROM1*, or *PKC1* plasmid into the *elp3Δ* strain partially suppressed the growth defect at 37°C (Fig 1A). No suppression of the phenotype was observed when the cells carried a high-copy *RHO1*, *BCK1* or *MPK1* plasmid (Fig 1A). As the overexpression of neither the upstream GTPase (Rho1) nor the downstream kinases (Bck1 and Mpk1) suppressed the Ts phenotype, we considered the possibility that the levels of these factors may be too high when expressed from a high-copy plasmid. Accordingly, low-copy *RHO1*, *BCK1* and *MPK1* plasmids suppress the Ts phenotype of *elp3Δ* cells to a level similar to that observed for the high-copy

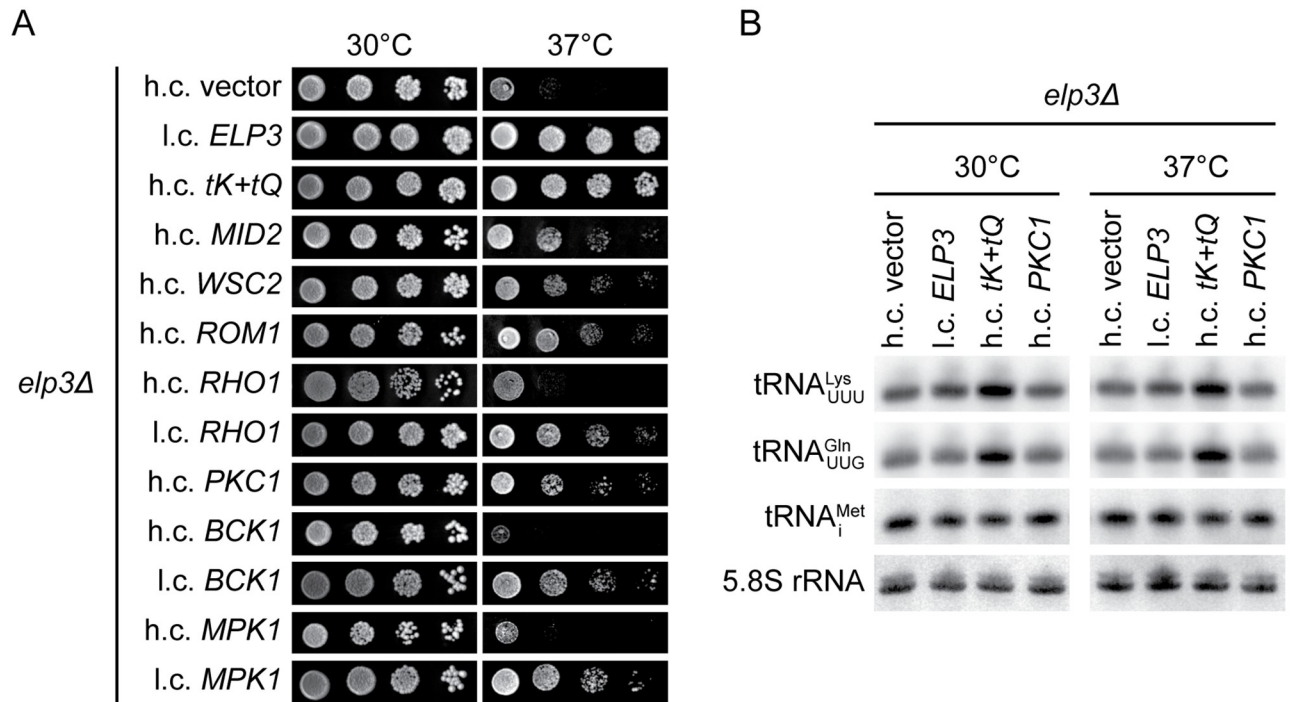


Fig 1. Increased expression of factors in the CWI signaling pathway counteracts the Ts phenotype of W303-derived *elp3Δ* cells. (A) Growth of the *elp3Δ* (UMY3269) strain carrying the indicated high-copy (h.c.) or low-copy (l.c.) *LEU2* plasmids. The high copy plasmid carrying the *tK(UUU)* and *tQ(UUG)* genes [74] is abbreviated as h.c. *tK+tQ*. Cells were grown over-night at 30°C in liquid synthetic complete medium lacking leucine (SC-leu), serially diluted, spotted on SC-leu plates, and incubated at 30°C or 37°C for 3 days. (B) Northern analysis of total RNA isolated from *elp3Δ* (UMY3269) cells carrying the indicated plasmids. The cells were grown in SC-leu medium at 30°C or 37°C. The blot was probed for tRNA^{Lys}_{UUU}, tRNA^{Gln}_{UUG}, tRNA^{Met}_i, and 5.8S rRNA using radiolabeled oligonucleotides. 5.8S rRNA serves as the loading control.

<https://doi.org/10.1371/journal.pgen.1008117.g001>

MID2, *WSC2*, *ROM1*, and *PKC1* plasmids (Fig 1A). The level of suppression is, however, smaller than that observed for increased *tK(UUU)* and *tQ(UUG)* dosage, encoding tRNA^{Lys}_{UUU} and tRNA^{Gln}_{UUG}, respectively (Fig 1A).

Since the Ts phenotype of *elp3Δ* cells is counteracted by elevated tRNA^{Lys}_{UUU} and tRNA^{Gln}_{UUG} levels [20], it was possible that the activation of the CWI pathway leads to an increase in their relative abundance. To investigate this possibility, we used northern blotting to analyze the effect of increased *PKC1* dosage on the levels of tRNA^{Lys}_{UUU} and tRNA^{Gln}_{UUG} in *elp3Δ* cells grown at either 30°C or 37°C. The blots were also probed for tRNA^{Met}_i and 5.8S rRNA, which served as the loading control. These RNAs were selected as tRNA^{Met}_i does not contain an Elongator-dependent tRNA modification and 5.8S rRNA is transcribed by a different RNA polymerase (RNA polymerase I). In contrast to the ≈2-fold increase in tRNA^{Lys}_{UUU} and tRNA^{Gln}_{UUG} levels induced by increased *tK(UUU)* and *tQ(UUG)* dosage (Fig 1B and S1 Table), the abundance of the tRNAs was largely unaffected by increased *PKC1* dosage at 30°C (Fig 1B and S1 Table). At 37°C, the increased *PKC1* dosage correlated with a slight increase in the levels of tRNA^{Lys}_{UUU} (Fig 1B and S1 Table). However, a similar effect was observed in the *elp3Δ* strain complemented with the *ELP3* gene, making it difficult to assess if the increase is the cause or the consequence of the improved growth at 37°C. Nevertheless, our results suggest that the Ts phenotype of *elp3Δ* cells is, at least in the W303 genetic background, partially suppressed by increased activation of the CWI signaling pathway.

The allelic variant at the *SSD1* locus modulates the growth phenotypes of *elp3Δ* cells

Phenotypes caused by a mutation in an individual gene can be modulated by the genetic background of the cell. In fact, the Ts phenotype induced by an *elp3Δ* allele is more pronounced in strains derived from W303 than in those from S288C (Fig 2A). As the inactivation of Elongator causes a lack of wobble mcm⁵/ncm⁵ groups in both strain backgrounds [5, 43], the Ts phenotype is likely modulated by genetic variation between W303 and S288C. The difference in phenotype (Fig 2A) prompted us to investigate if increased *MID2*, *WSC2*, *ROM1*, *RHO1*, *PKC1*, *BCK1* or *MPK1* dosage counteracts the Ts phenotype of *elp3Δ* cells in the S288C background. The analyses showed that none of the plasmids counteracted the phenotype (S1A Fig). Moreover, the growth defect of *elp3Δ* cells at 37°C is counteracted by osmotic support (1 M sorbitol) in the W303, but not in the S288C background (S1B Fig). Importantly, the Ts phenotype of *elp3Δ* cells is suppressed by increased *tK(UUU)* and *tQ(UUG)* dosage in both genetic backgrounds (Fig 1A and S1A Fig), showing that the underlying cause is the hypomodified tRNA^{Lys}_{UUU} and tRNA^{Gln}_{UUG}. We conclude that the genetic background influences the phenotypes linking the tRNA modification defect to cell wall integrity.

Although W303 is closely related to S288C, comparisons of the genomes identified polymorphisms in ≈800 genes that lead to variations in the amino acid sequence [44, 45]. To identify the cause of the phenotypic differences between the *elp3Δ* strains, we examined polymorphisms that have been shown to be physiologically relevant. The polymorphism at the *SSD1* locus was a good candidate as *SSD1* has been genetically implicated in many cellular processes, including the maintenance of cellular integrity [32, 33, 46–50]. Ssd1 is a RNA binding protein that associates with a subset of mRNAs of which many encode proteins important for cell wall biosynthesis and remodeling [26–28]. The *SSD1* allele in the S288C background encodes the full-length Ssd1 protein (1250 amino acids) whereas the allele in W303, designated *ssd1-d2*, contains a nonsense mutation that introduces a premature stop codon at the 698th codon of the open reading frame [32, 35]. To investigate if the allele at the *SSD1* locus contributes to the phenotypic differences between the *elp3Δ* mutants, we analyzed congenic *ssd1-d2*, *SSD1*, *ssd1-d2 elp3Δ*, and *SSD1 elp3Δ* strains in both genetic backgrounds. By analyzing the growth of the strains, we found that the *ssd1-d2* allele augments the Ts phenotype of *elp3Δ* cells in both backgrounds (Fig 2B and S2 Table). The *ssd1-d2* allele also appears to cause a slightly reduced growth rate of strains with a wild-type *ELP3* gene at the elevated temperature (S2 Table). Even though the *elp3Δ* mutants grow slower than the *ELP3* strains at 30°C, the effect of the *ssd1-d2* allele is less pronounced at that temperature (S2 Table). In both genetic backgrounds, the increased activation of the CWI signaling pathway, through increased *PKC1* dosage, suppresses the Ts phenotype of the *ssd1-d2 elp3Δ*, but not the *SSD1 elp3Δ* strains (Fig 2C). Although the *elp3Δ* strains show increased sensitivity to caffeine, irrespective of the allele at the *SSD1* locus, the *ssd1-d2 elp3Δ* cells are in both backgrounds more caffeine-sensitive than the *SSD1 elp3Δ* cells (Fig 2D). This observation is consistent with the previous finding that the *ssd1-d2* allele enhances the growth inhibitory effects of caffeine [32].

The inactivation of Elongator not only leads to increased sensitivity to caffeine, but also to other stress-inducing agents [14, 17, 18]. To investigate if the *ssd1-d2* allele influences these phenotypes, we analyzed the growth of the *ssd1-d2*, *SSD1*, *ssd1-d2 elp3Δ*, and *SSD1 elp3Δ* strains on medium containing rapamycin, hydroxyurea, or diamide. The analyses revealed that the *ssd1-d2* allele, irrespective of background, also increases the sensitivity of *elp3Δ* cells to these compounds (Fig 2D). To ensure that the effect of the *ssd1-d2* allele is not restricted to one set of congenic strains, we repeated the growth assays, in both genetic backgrounds, using a second set of *ssd1-d2*, *SSD1*, *ssd1-d2 elp3Δ*, and *SSD1 elp3Δ* isolates. The stress-induced

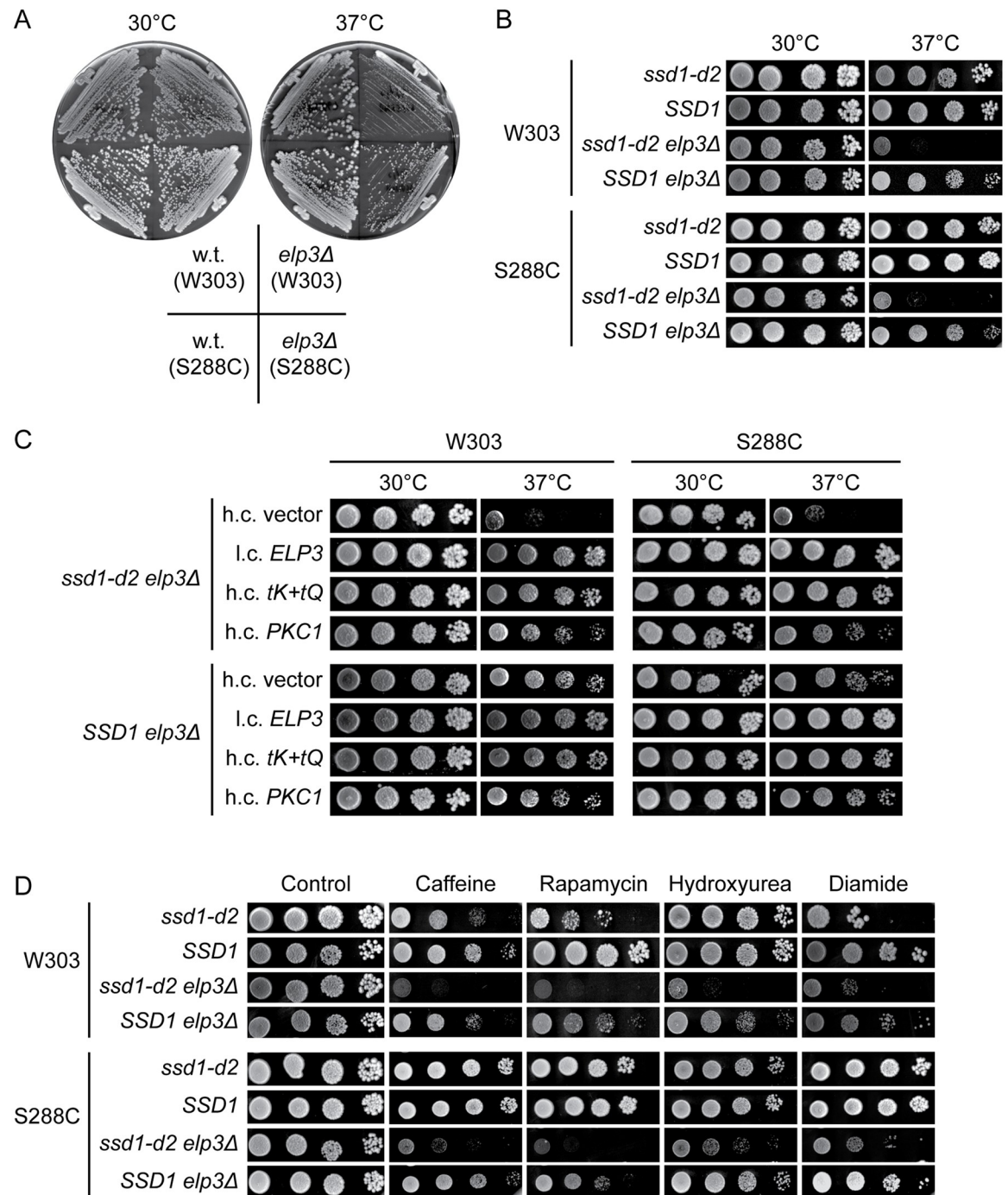


Fig 2. The growth phenotypes *elp3Δ* cells are modulated by the allele at the *SSD1* locus. (A) Growth of *elp3Δ* mutants in the W303 and S288C genetic backgrounds. The wild-type (W303-1A and BY4741) and *elp3Δ* strains (UMY3269 and MJY1036) were streaked on SC plates and incubated at 30°C or 37°C for 3 days. (B) Effects of the *ssd1-d2/SSD1* alleles on the growth of *elp3Δ* strains in the W303 and S288C genetic backgrounds. The *ssd1-d2* (W303-1A and UMY4432), *SSD1* (UMY3385 and BY4741), *ssd1-d2 elp3Δ* (UMY3269 and UMY4439) and *SSD1 elp3Δ* (UMY4456 and MJY1036) strains were grown over-night at 30°C in liquid SC medium, serially diluted, spotted on SC plates, and incubated at 30°C or 37°C for 3 days. (C) Effects of increased *PKC1* dosage on the growth of *elp3Δ ssd1-d2* and *elp3Δ SSD1* strains. The relevant strains (UMY3269, UMY4456, UMY4439, and MJY1036) carrying the indicated plasmids were grown over-night at 30°C in liquid SC-leu medium, serially diluted, spotted on SC-leu plates, and incubated for 3 days at 30°C or 37°C. (D) Influence of the *ssd1-d2* allele on growth phenotypes induced by various stress-inducing agents. The strains from B were grown over-night at 30°C in liquid SC medium, serially diluted, and spotted on SC plates and SC plates supplemented with caffeine, rapamycin, hydroxyurea or diamide. The plates were incubated for 3 days at 30°C.

<https://doi.org/10.1371/journal.pgen.1008117.g002>

growth defects of *elp3Δ* cells were also in these strains augmented by the *ssd1-d2* allele (S2 Fig). As translational readthrough of the premature stop codon in the *ssd1-d2* mRNA could generate low levels of full-length functional Ssd1 protein, we also investigated the effect of an *ssd1Δ* allele on the growth phenotypes of *elp3Δ* mutants. In both genetic backgrounds, the effect of the *ssd1Δ* allele is comparable to the *ssd1-d2* mutation (S3 Fig). Collectively, these results show that the allele at the *SSD1* locus influences stress-induced growth defects of *elp3Δ* cells.

Ssd1 does not appear to influence the abundance, modification, or function of tRNAs

As the phenotypes of Elongator mutants are largely caused by the reduced functionality of the hypomodified tRNA^{Lys}_{UUU} and tRNA^{Gln}_{UUG} [20], it seemed possible that the *ssd1-d2* allele may influence tRNA abundance or function. To investigate if the allele at the *SSD1* locus influence tRNA abundance, we used northern blotting to determine the levels of tRNA^{Lys}_{UUU}, tRNA^{Gln}_{UUG}, and tRNA^{Met}_i in the *ssd1-d2*, *SSD1*, *ssd1-d2 elp3Δ*, and *SSD1 elp3Δ* strains. The analyses revealed that the relative levels of the tRNAs are, in both genetic backgrounds, largely unaffected by the allelic variant at the *SSD1* locus (S4 Fig and S3 Table). Moreover, HPLC analyses of the nucleoside composition of total tRNA isolated from the strains showed that the levels of ncm⁵U, mcm⁵U, and mcm⁵s²U are comparable in the *ssd1-d2* and *SSD1* strains and not detectable in the *ssd1-d2 elp3Δ* and *SSD1 elp3Δ* mutants (S4 Table). The HPLC analyses also revealed that the allele at the *SSD1* locus has no apparent effect on the abundance of other modified nucleosides present in tRNAs (S5 Fig and S4 Table).

To investigate if the allele at the *SSD1* locus influences tRNA function, we utilized a +1 frameshifting reporter system [51, 52]. By using this system, it was previously shown that *elp3Δ* cells show elevated levels of +1 frameshifting on a CUU AAA C frameshifting site [52]. Further, this increase is caused by slow entry of the hypomodified tRNA^{Lys}_{UUU} into the ribosomal A-site and the consequent slippage of the P-site tRNA [52]. Although analyses of the *ssd1-d2*, *SSD1*, *ssd1-d2 elp3Δ*, and *SSD1 elp3Δ* strains confirmed that the *elp3Δ* mutants show elevated levels of +1 frameshifting on the CUU AAA C sequence, we detected no influence of the allele at the *SSD1* locus (Table 1). Thus, Ssd1 does not appear to influence the functionality of the hypomodified tRNA^{Lys}_{UUU}.

The *ssd1-d2* allele is required for the histone acetylation and telomeric gene silencing defects of *elp3Δ* mutants

In the W303 background, *elp3Δ* mutants show reduced acetylation of histone H3 [15]. Although the phenotype was originally thought to reflect a function of Elongator in RNA polymerase II transcription [15], the reduced acetylation of lysine-14 (K14) in histone H3 was

Table 1. The allele at the *SSD1* locus does not influence +1 frameshifting.

Strain	Percent frameshifting ^a
<i>ssd1-d2</i> (W303-1A)	0.32 ± 0.09
<i>ssd1-d2 elp3Δ</i> (UMY3269)	2.28 ± 0.33
<i>SSD1</i> (UMY3385)	0.20 ± 0.09
<i>SSD1 elp3Δ</i> (UMY4456)	2.61 ± 0.09

^a The value for the β-galactosidase activity in cells carrying the frameshift construct (CUU AAA C, pABY2139) was divided by the value for the in-frame control (pABY2144). The values represent the mean from four independent experiments. The standard deviation is indicated.

<https://doi.org/10.1371/journal.pgen.1008117.t001>

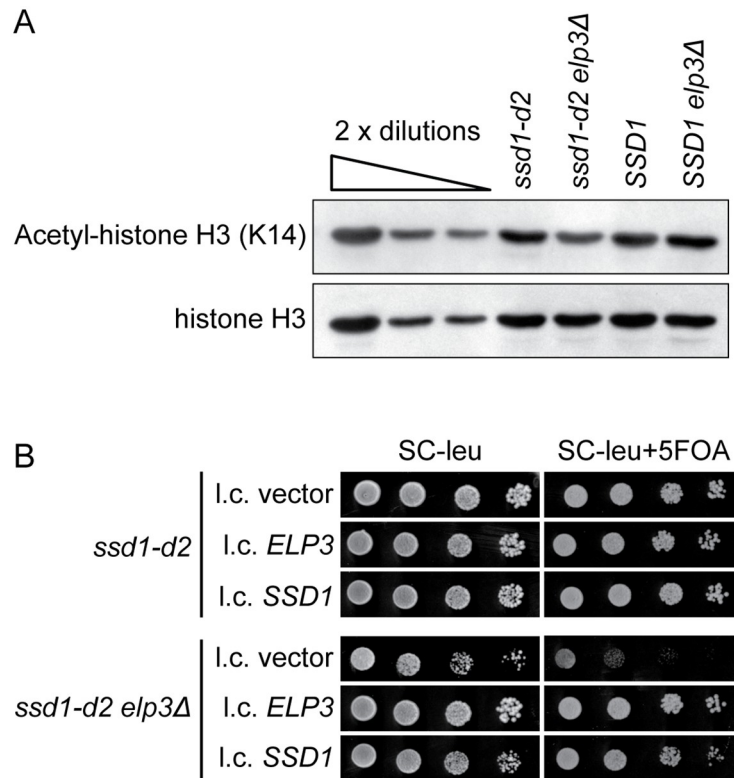


Fig 3. The *ssd1-d2* allele is required for the histone acetylation and telomeric gene silencing defects of *elp3Δ* cells. (A) Western analysis of histones isolated from the *ssd1-d2* (W303-1A), *ssd1-d2 elp3Δ* (UMY3269), *SSD1* (UMY3385) and *SSD1 elp3Δ* (UMY4456) strains grown in SC medium at 30°C. Polyclonal anti-acetyl-histone H3 and anti-histone H3 antibodies were used to detect the indicated proteins. The blot is a representative of three independent experiments. (B) Influence of the *ssd1-d2* allele on telomeric gene silencing in *elp3Δ* cells. The *ssd1-d2 TELVIII::URA3* (UMY2584) and *ssd1-d2 elp3Δ TELVIII::URA3* (UMY3790) strains carrying the indicated plasmids were grown overnight at 30°C in liquid SC-leu medium, serially diluted, spotted on SC-leu and SC-leu+5-FOA plates, and incubated for 3 days at 30°C.

<https://doi.org/10.1371/journal.pgen.1008117.g003>

subsequently shown to be an indirect consequence of the tRNA modification defect [20]. To investigate if the *ssd1-d2* allele contributes to the phenotype, we analyzed, in the W303 background, the histone H3 K14 acetylation levels in the *ssd1-d2*, *ssd1-d2 elp3Δ*, *SSD1*, and *SSD1 elp3Δ* strains. As previously shown [15, 20], the level of K14 acetylation is lower in the *ssd1-d2 elp3Δ* mutant than in the *ssd1-d2* strain (Fig 3A). However, the *SSD1* and *SSD1 elp3Δ* strains show comparable levels of K14 acetylated histone H3, indicating that it is the combination of the *elp3Δ* and *ssd1-d2* alleles that induces the histone H3 acetylation defect.

W303-derived Elongator mutants have also been reported to show delayed transcriptional activation of the *GAL1* and *GAL10* genes upon a shift from raffinose- to galactose-containing medium [20, 53]. To determine if the *ssd1-d2* allele influences this phenotype, we analyzed the induction of the *GAL1* mRNA in the W303-derived *ssd1-d2*, *ssd1-d2 elp3Δ*, *SSD1*, and *SSD1 elp3Δ* strains. Unexpectedly, we observed no obvious delay in the induction of *GAL1* transcripts in the *elp3Δ* strains regardless of the nature of the allele at the *SSD1* locus (S6 Fig). As the phenotype is thought to reflect a reduced ability of Elongator mutants to adapt to new growth conditions [53], it is possible that differences in media or the handling of the cultures can explain why *elp3Δ* cells show rapid *GAL1* induction in our experiments.

Another phenotype reported for Elongator mutants in the W303 background is a defect in telomeric gene silencing [17, 21]. The telomere silencing defect of Elongator mutants was inferred from experiments where the expression of a *URA3* gene integrated close to the left telomere of chromosome VII was assayed [17, 21]. The defect in telomeric gene silencing leads to increased expression of the *URA3* gene, which is scored as reduced growth on plates containing 5-fluoroorotic acid (5-FOA) [17, 21]. Even though the integration of an *SSD1* allele into *ssd1-d2* cells does not influence the level of telomeric gene silencing [36], the inactivation of *SSD1* does increase the expression of a reporter gene at the silent mating type locus HMR [54]. The latter finding implies that the *ssd1-d2* allele may influence the assembly of silent chromatin and consequently contribute to the silencing defect in Elongator mutants. Accordingly, the introduction of a low-copy *SSD1* plasmid into the *ssd1-d2 elp3Δ TELVIII::URA3* strain [21] complemented the 5-FOA sensitivity to a level similar to that observed with a plasmid carrying the wild-type *ELP3* gene (Fig 3B). Thus, the telomeric gene silencing defect in Elongator mutants is caused by a synergistic interaction between the *ssd1-d2* and *elp3Δ* alleles.

The *ssd1-d2* allele augments phenotypes induced by the simultaneous lack of *mcm⁵* and *s²* groups

In the formation of *mcm⁵s²U₃₄*, Elongator promotes synthesis of the *mcm⁵* side-chain whereas the thiolation of the 2-position is catalyzed by the Ncs2/Ncs6 complex [40, 43, 55–57]. The simultaneous lack of *mcm⁵* and *s²* groups was originally reported to be lethal [40]. However, those experiments were performed in the W303 background and more recent studies have shown that strains lacking both groups are viable in the S288C background [18, 41]. To investigate if the allele at the *SSD1* locus accounts for the difference in viability, we constructed *ssd1-d2 elp3Δ ncs2Δ* and *SSD1 elp3Δ ncs2Δ* strains in both backgrounds all carrying a wild-type *ELP3* gene on a low-copy *URA3* plasmid. Analyses of the strains revealed that the *elp3Δ ncs2Δ* double mutant is viable in the W303 background if it encompasses an *SSD1* allele (Fig 4A; S7 Fig shows the same plates after a 2-day incubation). In the S288C background, the *ssd1-d2 elp3Δ ncs2Δ* strain is viable but it grows slower than the *SSD1 elp3Δ ncs2Δ* strain (Fig 4A and 4B). These observations not only show that allele at the *SSD1* locus influences the viability of *elp3Δ ncs2Δ* cells, but they also indicate that the growth phenotype is modulated by additional genetic factors.

The lack of the *mcm⁵* and/or *s²* groups has, in the S288C background, been shown to correlate with an increased accumulation of protein aggregates [18]. This effect was most pronounced in a strain lacking both groups and the phenotype was suggested to be a consequence of co-translational misfolding due to slower decoding of AAA and CAA codons by the hypomodified tRNA^{Lys}_{UUU} and tRNA^{Gln}_{UUG} [18]. Moreover, the increased load of aggregates during normal growth was proposed to account for observation that the double mutant is impaired in clearing diamide-induced protein aggregates [18]. As strains deleted for *SSD1* show a defect in the disaggregation of heat-shock-induced protein aggregates [58], it seemed possible that the *ssd1-d2* allele would augment the protein homeostasis defect in *elp3Δ ncs2Δ* cells. To investigate this possibility, we isolated aggregates [18, 59] from the *ssd1-d2*, *SSD1*, *ssd1-d2 elp3Δ ncs2Δ*, and *SSD1 elp3Δ ncs2Δ* strains. Analyses of the insoluble fractions revealed that the levels of aggregated proteins are comparable in the *ssd1-d2* and *SSD1* strains (Fig 4C). However, the *ssd1-d2 elp3Δ ncs2Δ* mutant shows increased accumulation of aggregates compared to the *SSD1 elp3Δ ncs2Δ* strain (Fig 4C). Thus, the allele at the *SSD1* locus modulates the protein homeostasis defect induced by the simultaneous lack of the wobble *mcm⁵* and *s²* groups.

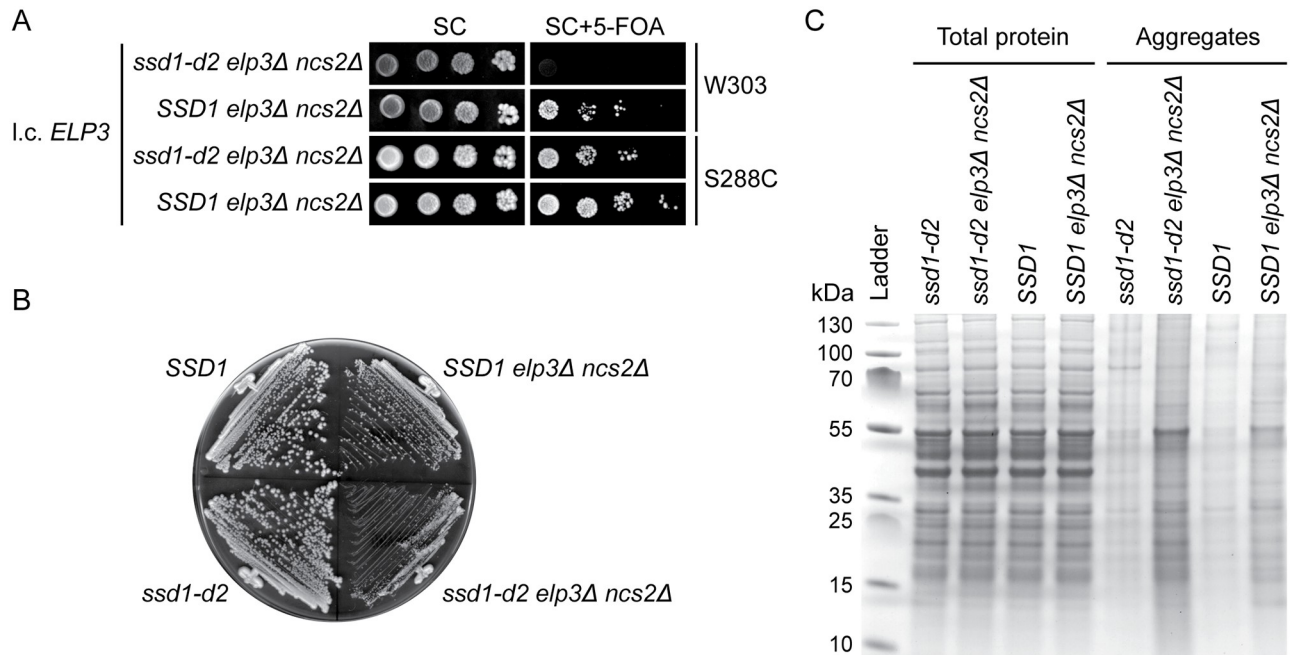


Fig 4. The growth and protein homeostasis defects of *elp3Δ ncs2Δ* cells are augmented by the *ssd1-d2* allele. (A) Influence of the *ssd1-d2* allele on the growth of *elp3Δ ncs2Δ* cells. The *ssd1-d2 elp3Δ ncs2Δ* (UMY4454 and MJY1159) and *SSD1 elp3Δ ncs2Δ* (UMY4467 and MJY1058) strains carrying the i.c. *URA3* plasmid pRS316-*ELP3* were grown over-night at 30°C in SC medium, serially diluted, spotted on SC and SC+5-FOA plates, and incubated for 3 days at 30°C. (B) Growth of S288C-derived *SSD1 elp3Δ ncs2Δ* and *ssd1-d2 elp3Δ ncs2Δ* strains. The wild-type (BY4741 and UMY4432) and *elp3Δ ncs2Δ* strains (MJY1058 and UMY4449) were streaked on a SC plate and incubated at 30°C for 2 days. (C) Effects of the *ssd1-d2* allele on protein aggregation in *elp3Δ ncs2Δ* cells. Total protein and protein aggregates was analyzed from the *ssd1-d2* (UMY4432), *ssd1-d2 elp3Δ ncs2Δ* (UMY4449), *SSD1* (BY4741) and *SSD1 elp3Δ ncs2Δ* (MJY1058) strains grown in SC medium at 30°C. The gel is a representative of two independent experiments.

<https://doi.org/10.1371/journal.pgen.1008117.g004>

Discussion

The phenotypic penetrance of a mutation is often impacted by the genetic background, a phenomenon frequently observed in monogenic diseases [60, 61]. In this study, we investigate the effect of genetic background on the phenotypes of *S. cerevisiae* mutants defective in the formation of modified wobble uridines in tRNAs. We show that the phenotypes of Elongator mutants are augmented by the *ssd1-d2* allele found in some wild-type laboratory strains. Moreover, the histone H3 acetylation and telomeric gene silencing defects reported for Elongator mutants are only observed in cells harboring the *ssd1-d2* allele. Thus, the *ssd1-d2* allele sensitizes yeast cells to the effects induced by the lack of *mcm*⁵/*ncm*⁵ groups in U₃₄-containing tRNAs.

Although the pleiotropic phenotypes of Elongator mutants are largely caused by the reduced functionality of the hypomodified tRNA^{Lys}_{UUU}, tRNA^{Gln}_{UUG} and tRNA^{Glu}_{UUC}, the basis for individual phenotypes is poorly understood. Several not necessarily mutually exclusive models have been proposed to explain how the lack of the *mcm*⁵/*ncm*⁵ groups can lead to a particular phenotype. One model postulates that phenotypes can be induced by inefficient translation of mRNAs enriched for AAA, CAA and/or GAA codons and the consequent effects on the abundance of the encoded factors [21, 62–64]. In this model, the inefficient decoding of the mRNAs leads to reduced protein output without affecting transcript abundance. The mechanism by which the slower decoding of the codons leads to reduced protein levels is unclear, but it may involve the inhibition of translation initiation by the queuing of ribosomes. Alternative models suggest that the phenotypes can be caused by defects in protein homeostasis and/

or by indirect effects on transcription [18, 22]. The inactivation of *SSD1* not only influences translation and stability of the transcripts normally bound by Ssd1, but it also leads to altered abundance of many transcripts that do not appear to be Ssd1-associated [28, 39]. Thus, the effects of the *ssd1-d2* allele on the phenotypes of *elp3Δ* cells could be due to either direct or indirect effects on gene expression. Moreover, the ribosome profiling experiments of Elongator mutants have been performed in the S288C background [18, 22, 23] and it remains possible that the lack of Ssd1 influences decoding of the AAA, CAA, and GAA codons. However, we observed no apparent effect of the *ssd1-d2* allele on the +1 frameshifting induced by the lack of Elongator (Table 1), indicating that Ssd1 does not influence the A-site selection rate.

While the difference at the *SSD1* locus partially explains the nonviability of *elp3Δ ncs2Δ* cells in the W303 background, the W303-derived *SSD1 elp3Δ ncs2Δ* strain grows slower than the corresponding strain in the S288C background (S7 Fig). Moreover, the *ssd1-d2 elp3Δ ncs2Δ* strain is viable, although with a growth defect, in the S288C background. These findings indicate that the growth phenotypes of *elp3Δ ncs2Δ* cells strains are modulated by additional genetic factors. Consistent with the finding that *ssd1Δ* cells show a defect in Hsp104-mediated protein disaggregation [58], the *ssd1-d2 elp3Δ ncs2Δ* strain shows increased accumulation of protein aggregates compared to the *SSD1 elp3Δ ncs2Δ* strain in the S288C background (Fig 4C). It is, however, unclear if this increase is the cause or the consequence of the reduced growth of the *ssd1-d2 elp3Δ ncs2Δ* strain.

Materials and methods

Yeast strains, plasmids, media and genetic procedures

Strains and plasmids used in this study are listed in S5 and S6 Tables. Yeast media were prepared as described [65, 66]. The medium was where appropriate supplemented with 2.5 ng/ml rapamycin (R0395, Sigma-Aldrich), 7 mM caffeine (C0750, Sigma-Aldrich), 100 mM hydroxyurea (H8627, Sigma-Aldrich), 0.25 mg/ml diamide (D3648, Sigma-Aldrich), or 1 mg/ml 5-fluoroorotic acid (R0812, Thermo Fisher).

To generate *ssd1-d2* derivatives of BY4741 and BY4742 (S288C background) [67], we first replaced the sequence between position 2907 and 3315 of the *SSD1* ORF with a *URA3* gene PCR-amplified from pRS316 [68]. The oligonucleotides used for strain constructions are described in S7 Table. The generated strains were transformed with an *ssd1-d2* DNA fragment PCR-amplified from W303-1A [69]. Following selection on 5-fluoroorotic acid (5-FOA)-containing plates and subsequent single cell streaks, individual clones were screened for the integration of *ssd1-d2* allele by PCR and DNA sequencing. The generated strains (UMY4432 and UMY4433) were allowed to mate producing the homozygous *ssd1-d2/ssd1-d2* strain (UMY4434).

Strains deleted for *SSD1*, *ELP3*, or *NCS2* were constructed by transforming the appropriate diploid (UMY3387, UMY2836 or UMY4434) with an *ssd1::KanMX4*, *elp3::KanMX4*, or *ncs2::KanMX4* DNA fragment with appropriate homologies. The DNA fragments were PCR-amplified from *ssd1::KanMX4* (Open Biosystems deletion collection), *elp3::KanMX4* (UMY3269), or *ncs2::KanMX4* (UMY3442) strains. Following PCR confirmation of the deletion, the generated heterozygous diploids were allowed to sporulate and the W303 *ssd1Δ* (UMY4558), S288C *ssd1Δ* (UMY4559), W303 *elp3Δ SSD1* (UMY4456 and UMY4457), W303 *ncs2Δ SSD1* (MJY1019), S288C *elp3Δ ssd1-d2* (UMY4438 and UMY4439), S288C *ncs2Δ ssd1-d2* (UMY4442), S288C *elp3Δ SSD1* (MJY1036), and S288C *ncs2Δ SSD1* (MJY1021) strains were obtained from tetrads. The *ssd1Δ elp3Δ* mutants (MJY1227 and UMY4574) were obtained from crosses between the relevant *ssd1Δ* and *elp3Δ* strains. The *elp3Δ ncs2Δ SSD1* mutants (MJY1058 and UMY4467) were obtained from crosses between the relevant strains. The

diploids used to generate the *elp3Δ ncs2Δ ssd1-d2* strains (MJY1159 and UMY4454) were transformed with pRS316-*ELP3* [40] before sporulation. MJY1159 was able to lose the plasmid generating strain UMY4449.

To construct plasmids carrying individual genes for factors in the CWI signaling pathway, we PCR-amplified the gene of interest using oligonucleotides that introduce appropriate restriction sites (S7 Table). The DNA fragment was then cloned into the corresponding sites of pRS425 [70] or pRS315 [68].

RNA methods

The abundance of individual tRNA species was determined in total RNA isolated from exponentially growing cultures at an optical density at 600 nm (OD_{600}) of ≈ 0.5 [66]. Samples containing 10 μ g of total RNA were separated on 8M urea-containing 8% polyacrylamide gels followed by electroblotting to Zeta-probe membranes (Bio-Rad). The blots were sequentially probed for tRNA^{Lys}_{UUU}, tRNA^{Gln}_{UUG}, tRNA^{Met}_i, and 5.8S rRNA using ³²P-labeled oligonucleotides (S7 Table). Signals were detected and analyzed by phosphorimaging using a Typhoon FLA 9500 biomolecular imager and Quantity One software.

To analyze the induction of *GAL1* transcripts, cells were grown at 30°C in 50 ml synthetic complete (SC) medium containing 2% raffinose (SC/Raf) to $OD_{600} \approx 0.45$. The culture was harvested by centrifugation at 1,500 x g for 5 min at room temperature, and the cell pellet resuspended in 15 ml pre-warmed (30°C) SC/Raf medium. Following reincubation in the shaking water bath for 10 min, transcription of *GAL1* was induced by the addition of 1.5 ml pre-warmed 20% galactose. Aliquots were harvested [66] at various time points after the addition of galactose and the cell pellets frozen on dry ice. The procedures for determining mRNA levels have been described [66].

To analyze the nucleoside composition of total tRNA, the tRNA was isolated from exponentially growing cultures at $OD_{600} \approx 0.8$ [21]. The tRNA was digested to nucleosides using nuclease P1 (Sigma-Aldrich, N8630) and bacterial alkaline phosphatase (Sigma-Aldrich, P4252) and the hydrolysate analyzed by HPLC [71, 72]. The compositions of the elution buffers were as described [72] with the difference that methanol concentration in buffer A was changed to 5% (v/v).

β -galactosidase assays

Cells transformed with pABY2139 or pABY2144 were grown in synthetic complete medium lacking uracil (SC-ura) to $OD_{600} \approx 0.5$. Cells representing 10 OD units were harvested and the β -galactosidase activity determined in protein extracts as described previously [65]. The +1 frameshifting levels were determined by dividing the β -galactosidase activity in extracts of cells containing the frameshift construct (pABY2139) with that of cells containing the in-frame control (pABY2144).

Histone preparation and immunoblot analyses

Histones were isolated from cells grown in SC medium at 30°C to $OD_{600} \approx 0.8$. Cells representing 100 OD_{600} units were harvested, washed once with water, resuspended in 30 ml of buffer A (0.1 mM Tris-HCl at pH 9.4, 10 mM DTT), and incubated on a rotator at 30°C for 15 min. Cells were collected, washed with 30 ml buffer B (1 M Sorbitol, 20 mM HEPES at pH 7.4) and resuspended in 25 ml of buffer B containing 600 U yeast lytic enzyme. After 1 hour incubation on a rotator at 30°C, the sample was mixed with 25 ml of ice-cold buffer C (1 M Sorbitol, 20 mM PIPES at pH 6.8, 1 mM MgCl₂) followed by centrifugation at 1,500 x g for 5 min. The pellet was resuspended in 40 ml nuclei isolation buffer [73] and the suspension incubated with

gentle mixing at 4°C for 30 min. Cell debris were removed by centrifugation at 1,500 x g for 5 min. The supernatant was homogenized with 5 strokes in a Dounce homogenizer followed by centrifugation at 20,000 x g for 10 min. Histones in the pelleted nuclei were extracted by re-suspension in 5 ml of cold 0.2 M H₂SO₄ and overnight incubation on a rotator at 4°C. After centrifugation at 10,000 x g for 10 min, proteins in the supernatant were precipitated by adding 0.5 volumes of 100% trichloroacetic and 30 min of incubation on ice. Following centrifugation, the pellet was washed twice with acetone and then dissolved in 200 µl 10 mM Tris-HCl at pH 8.0. Fractions (10 µl) were resolved by 15% SDS-PAGE and transferred to Immobilon-P (Millipore) membranes. The blots were incubated with rabbit anti-acetyl-histone H3 (Lys14) antibodies (1:1,000 dilution, Millipore, 07–353) and then with horseradish peroxidase-linked donkey anti-rabbit IgG (NA934, GE Healthcare). Blots were stripped and reprobed with rabbit anti-histone H3 antibodies (1:5,000 dilution, Millipore, 07–690). Proteins were detected using ECL Western blotting detection reagents (GE Healthcare, RPN2209) and Amersham Hyperfilm ECL (GE Healthcare, 28906836).

Analysis of protein aggregates

Protein aggregates were analyzed in exponentially growing cultures in SC medium at 30°C. Cells representing 50 OD₆₀₀ units were harvested at OD₆₀₀≈0.5 and protein aggregates were isolated [18, 59] from samples containing 5 mg of total protein. 1/10 of the aggregates and 5µg of total protein were resolved on a 4–12% NuPAGE Bis-Tris gel (Thermo Fisher, NP0321BOX) followed by staining with the Colloidal Blue Staining Kit (Thermo Fisher, LC6025).

Supporting information

S1 Fig. The S288C-derived *elp3Δ* strain does not appear to have cell wall integrity defect.

(A) Growth of the *elp3Δ* (MJY1036) strain carrying the indicated high-copy (h.c.) or low-copy (l.c.) *LEU2* plasmids. Cells were grown over-night at 30°C in liquid SC-leu medium, serially diluted, spotted on SC-leu plates, and incubated at 30°C or 37°C for 3 days. (B) The wild-type (W303-1A and BY4741) and *elp3Δ* (UMY3269 and MJY1036) strains were grown over-night at 30°C in liquid SC medium, serially diluted, and spotted on SC plates and SC plates supplemented with 1M sorbitol. The plates were incubated for 3 days at 30°C or 37°C.

(PDF)

S2 Fig. The allele at the *SSD1* locus modulates the growth phenotypes of *elp3Δ* mutants in a second set of isolates.

The *ssd1-d2* (W303-1B and UMY4433), *SSD1* (UMY3386 and BY4742), *ssd1-d2 elp3Δ* (UMY2843 and UMY4438) and *SSD1 elp3Δ* (UMY4457 and MJY1037) strains were grown over-night at 30°C in liquid SC medium, serially diluted, and spotted on SC plates and SC plates supplemented with caffeine, rapamycin, hydroxyurea, or diamide. The plates were incubated at 30°C or 37°C for 3 days.

(PDF)

S3 Fig. The *ssd1-d2* and *ssd1Δ* alleles have similar effects on the growth phenotypes of *elp3Δ* mutants.

The *ssd1-d2* (W303-1A and UMY4432), *ssd1Δ* (UMY4558 and UMY4559), *SSD1* (UMY3385 and BY4741), *ssd1-d2 elp3Δ* (UMY3269 and UMY4439), *ssd1Δ elp3Δ* (UMY4574 and MJY1227), and *SSD1 elp3Δ* (UMY4456 and MJY1036) strains were grown over-night at 30°C in liquid SC medium, serially diluted, and spotted on SC plates and SC plates supplemented with caffeine, rapamycin, hydroxyurea, or diamide. The plates were incubated for 3 days at 30°C or 37°C.

(PDF)

S4 Fig. Effects of *ssd1-d2* and *SSD1* alleles on tRNA abundance. Northern analysis of total RNA isolated from the *ssd1-d2* (W303-1A and UMY4432), *ssd1-d2 elp3Δ* (UMY3269 and UMY4439), *SSD1* (UMY3385 and BY4741), and *SSD1 elp3Δ* (UMY4456 and MJY1036) strains grown in SC medium at 30°C. The blot was probed for tRNA_{UUU}^{Lys}, tRNA_{UUG}^{Gln}, tRNA_I^{Met}, and 5.8S rRNA using radiolabeled oligonucleotides.

(PDF)

S5 Fig. HPLC analyses of the nucleoside composition of total tRNA from various *ssd1-d2* and *SSD1* strains. The peaks representing ncm⁵U, mcm⁵U, mcm⁵s²U, pseudouridine (Ψ), cytidine (C), uridine (U), guanosine (G), adenosine (A), 1-methyladenosine (m¹A), 5-methylcytidine (m⁵C), 2'-O-methylcytidine (Cm), 1-methylguanosine (m¹G), N²-methylguanosine (m²G), N⁴-acetylcytidine (ac⁴C), and N², N²-dimethylguanosine (m₂²G) are indicated. The asterisk indicates a peak that is a contamination from the bacterial alkaline phosphatase.

(PDF)

S6 Fig. The transcriptional activation of *GAL1* is not impaired in *elp3Δ* mutants. Northern analysis of total RNA isolated from the *ssd1-d2* (W303-1A), *ssd1-d2 elp3Δ* (UMY3269), *SSD1* (UMY3385) and *SSD1 elp3Δ* (UMY4456) strains. Cells were grown in SC medium containing 2% raffinose followed by induction of *GAL1* transcription by the addition of 0.1 volumes 20% galactose. Time points after the addition of galactose are indicated above the lanes. The blot was probed for *GAL1* transcripts using a randomly labelled DNA fragment. 18S rRNA was detected using an oligonucleotide probe. The blot is a representative of two independent experiments.

(PDF)

S7 Fig. Influence of the *ssd1-d2* allele on the growth of *elp3Δ ncs2Δ* cells. The figure shows a shorter incubation (2 days) of the plates in [Fig 4A](#).

(PDF)

S1 Table. Steady-state tRNA levels in *elp3Δ* cells carrying the indicated plasmids.

(DOCX)

S2 Table. Generation times of indicated strains grown at 30°C or 37°C.

(DOCX)

S3 Table. Steady-state tRNA levels in the indicated strains.

(DOCX)

S4 Table. Relative amounts of selected modified nucleosides in total tRNA from various strains.

(DOCX)

S5 Table. Yeast strains used in this study.

(DOCX)

S6 Table. Plasmids used in this study.

(DOCX)

S7 Table. Oligonucleotides used in this study.

(DOCX)

Acknowledgments

We thank members of M.J.'s and A.B.'s laboratories for valuable discussions.

Author Contributions

Conceptualization: Fu Xu, Anders S. Byström, Marcus J. O. Johansson.

Formal analysis: Fu Xu, Marcus J. O. Johansson.

Funding acquisition: Anders S. Byström, Marcus J. O. Johansson.

Investigation: Fu Xu, Marcus J. O. Johansson.

Project administration: Anders S. Byström, Marcus J. O. Johansson.

Supervision: Anders S. Byström, Marcus J. O. Johansson.

Writing – original draft: Fu Xu, Marcus J. O. Johansson.

Writing – review & editing: Fu Xu, Anders S. Byström, Marcus J. O. Johansson.

References

1. Björk GR, Hagervall TG. Transfer RNA Modification: Presence, Synthesis, and Function. *EcoSal Plus*. 2014; 6. <https://doi.org/10.1128/ecosalplus.ESP-0007-2013> PMID: 26442937
2. Agris PF, Narendran A, Sarachan K, Vare VYP, Eruysal E. The Importance of Being Modified: The Role of RNA Modifications in Translational Fidelity. *Enzymes*. 2017; 41: 1–50. <https://doi.org/10.1016/bs.enz.2017.03.005> PMID: 28601219
3. Machnicka MA, Olchowiak A, Grosjean H, Bujnicki JM. Distribution and frequencies of post-transcriptional modifications in tRNAs. *RNA Biol*. 2014; 11: 1619–29. <https://doi.org/10.4161/15476286.2014.992273> PMID: 25611331
4. Phizicky EM, Hopper AK. tRNA biology charges to the front. *Genes Dev*. 2010; 24: 1832–60. <https://doi.org/10.1101/gad.1956510> PMID: 20810645
5. Huang B, Johansson MJO, Byström AS. An early step in wobble uridine tRNA modification requires the Elongator complex. *RNA*. 2005; 11: 424–36. <https://doi.org/10.1261/rna.7247705> PMID: 15769872
6. Winkler GS, Petrakis TG, Ethelberg S, Tokunaga M, Erdjument-Bromage H, Tempst P, et al. RNA polymerase II elongator holoenzyme is composed of two discrete subcomplexes. *J Biol Chem*. 2001; 276: 32743–9. <https://doi.org/10.1074/jbc.M105303200> PMID: 11435442
7. Dauden MI, Jaciuk M, Muller CW, Glatt S. Structural asymmetry in the eukaryotic Elongator complex. *FEBS Lett*. 2018; 592: 502–15. <https://doi.org/10.1002/1873-3468.12865> PMID: 28960290
8. Kolaj-Robin O, Seraphin B. Structures and Activities of the Elongator Complex and Its Cofactors. *Enzymes*. 2017; 41: 117–49. <https://doi.org/10.1016/bs.enz.2017.03.001> PMID: 28601220
9. Johansson MJO, Xu F, Byström AS. Elongator-a tRNA modifying complex that promotes efficient translational decoding. *Biochim Biophys Acta Gene Regul Mech*. 2018; 1861: 401–8. <https://doi.org/10.1016/j.bbagr.2017.11.006> PMID: 29170010
10. Kalhor HR, Clarke S. Novel methyltransferase for modified uridine residues at the wobble position of tRNA. *Mol Cell Biol*. 2003; 23: 9283–92. <https://doi.org/10.1128/MCB.23.24.9283-9292.2003> PMID: 14645538
11. Mazauric MH, Dirick L, Purushothaman SK, Björk GR, Lapeyre B. Trm112p is a 15-kDa zinc finger protein essential for the activity of two tRNA and one protein methyltransferases in yeast. *J Biol Chem*. 2010; 285: 18505–15. <https://doi.org/10.1074/jbc.M110.113100> PMID: 20400505
12. Chen C, Huang B, Anderson JT, Byström AS. Unexpected accumulation of mcm(5)U and mcm(5)S(2) (U) in a trm9 mutant suggests an additional step in the synthesis of mcm(5)U and mcm(5)S(2)U. *PLoS One*. 2011; 6: e20783. <https://doi.org/10.1371/journal.pone.0020783> PMID: 21687733
13. Karlsborn T, Tukenmez H, Mahmud AK, Xu F, Xu H, Byström AS. Elongator, a conserved complex required for wobble uridine modifications in eukaryotes. *RNA Biol*. 2014; 11: 1519–28. <https://doi.org/10.4161/15476286.2014.992276> PMID: 25607684
14. Frohloff F, Fichtner L, Jablonowski D, Breunig KD, Schaffrath R. *Saccharomyces cerevisiae* Elongator mutations confer resistance to the *Kluyveromyces lactis* zymocin. *EMBO J*. 2001; 20: 1993–2003. <https://doi.org/10.1093/emboj/20.8.1993> PMID: 11296232
15. Winkler GS, Kristjuhan A, Erdjument-Bromage H, Tempst P, Sveistrup JQ. Elongator is a histone H3 and H4 acetyltransferase important for normal histone acetylation levels in vivo. *Proc Natl Acad Sci U S A*. 2002; 99: 3517–22. <https://doi.org/10.1073/pnas.022042899> PMID: 11904415

16. Rahl PB, Chen CZ, Collins RN. Eip1p, the yeast homolog of the FD disease syndrome protein, negatively regulates exocytosis independently of transcriptional elongation. *Mol Cell*. 2005; 17: 841–53. <https://doi.org/10.1016/j.molcel.2005.02.018> PMID: 15780940
17. Li Q, Fazly AM, Zhou H, Huang S, Zhang Z, Stillman B. The elongator complex interacts with PCNA and modulates transcriptional silencing and sensitivity to DNA damage agents. *PLoS Genet*. 2009; 5: e1000684. <https://doi.org/10.1371/journal.pgen.1000684> PMID: 19834596
18. Nedialkova DD, Leidel SA. Optimization of Codon Translation Rates via tRNA Modifications Maintains Proteome Integrity. *Cell*. 2015; 161: 1606–18. <https://doi.org/10.1016/j.cell.2015.05.022> PMID: 26052047
19. Johansson MJO, Esberg A, Huang B, Björk GR, Byström AS. Eukaryotic wobble uridine modifications promote a functionally redundant decoding system. *Mol Cell Biol*. 2008; 28: 3301–12. <https://doi.org/10.1128/MCB.01542-07> PMID: 18332122
20. Esberg A, Huang B, Johansson MJO, Byström AS. Elevated levels of two tRNA species bypass the requirement for elongator complex in transcription and exocytosis. *Mol Cell*. 2006; 24: 139–48. <https://doi.org/10.1016/j.molcel.2006.07.031> PMID: 17018299
21. Chen C, Huang B, Eliasson M, Ryden P, Byström AS. Elongator complex influences telomeric gene silencing and DNA damage response by its role in wobble uridine tRNA modification. *PLoS Genet*. 2011; 7: e1002258. <https://doi.org/10.1371/journal.pgen.1002258> PMID: 21912530
22. Zinshteyn B, Gilbert WV. Loss of a conserved tRNA anticodon modification perturbs cellular signaling. *PLoS Genet*. 2013; 9: e1003675. <https://doi.org/10.1371/journal.pgen.1003675> PMID: 23935536
23. Chou HJ, Donnard E, Gustafsson HT, Garber M, Rando OJ. Transcriptome-wide Analysis of Roles for tRNA Modifications in Translational Regulation. *Mol Cell*. 2017; 68: 978–92 e4. <https://doi.org/10.1016/j.molcel.2017.11.002> PMID: 29198561
24. Levin DE. Cell wall integrity signaling in *Saccharomyces cerevisiae*. *Microbiol Mol Biol Rev*. 2005; 69: 262–91. <https://doi.org/10.1128/MMBR.69.2.262-291.2005> PMID: 15944456
25. Levin DE. Regulation of cell wall biogenesis in *Saccharomyces cerevisiae*: the cell wall integrity signaling pathway. *Genetics*. 2011; 189: 1145–75. <https://doi.org/10.1534/genetics.111.128264> PMID: 22174182
26. Uesono Y, Toh-e A, Kikuchi Y. Ssd1p of *Saccharomyces cerevisiae* associates with RNA. *J Biol Chem*. 1997; 272: 16103–9. <https://doi.org/10.1074/jbc.272.26.16103> PMID: 9195905
27. Hogan DJ, Riordan DP, Gerber AP, Herschlag D, Brown PO. Diverse RNA-binding proteins interact with functionally related sets of RNAs, suggesting an extensive regulatory system. *PLoS Biol*. 2008; 6: e255. <https://doi.org/10.1371/journal.pbio.0060255> PMID: 18959479
28. Jansen JM, Wanless AG, Seidel CW, Weiss EL. Cbk1 regulation of the RNA-binding protein Ssd1 integrates cell fate with translational control. *Curr Biol*. 2009; 19: 2114–20. <https://doi.org/10.1016/j.cub.2009.10.071> PMID: 19962308
29. Ohya Y, Kasahara K, Kokubo T. *Saccharomyces cerevisiae* Ssd1p promotes CLN2 expression by binding to the 5'-untranslated region of CLN2 mRNA. *Genes Cells*. 2010; 15: 1169–88. <https://doi.org/10.1111/j.1365-2443.2010.01452.x> PMID: 20977549
30. Wanless AG, Lin Y, Weiss EL. Cell morphogenesis proteins are translationally controlled through UTRs by the Ndr/LATS target Ssd1. *PLoS One*. 2014; 9: e85212. <https://doi.org/10.1371/journal.pone.0085212> PMID: 24465507
31. Kurischko C, Kim HK, Kuravi VK, Pratzka J, Luca FC. The yeast Cbk1 kinase regulates mRNA localization via the mRNA-binding protein Ssd1. *J Cell Biol*. 2011; 192: 583–98. <https://doi.org/10.1083/jcb.201011061> PMID: 21339329
32. Sutton A, Immanuel D, Arndt KT. The SIT4 protein phosphatase functions in late G1 for progression into S phase. *Mol Cell Biol*. 1991; 11: 2133–48. <https://doi.org/10.1128/mcb.11.4.2133> PMID: 1848673
33. Kaerberlein M, Guarente L. *Saccharomyces cerevisiae* MPT5 and SSD1 function in parallel pathways to promote cell wall integrity. *Genetics*. 2002; 160: 83–95. PMID: 11805047
34. Wilson RB, Brenner AA, White TB, Engler MJ, Gaughran JP, Tatchell K. The *Saccharomyces cerevisiae* SRK1 gene, a suppressor of bcy1 and ins1, may be involved in protein phosphatase function. *Mol Cell Biol*. 1991; 11: 3369–73. <https://doi.org/10.1128/mcb.11.6.3369> PMID: 1645449
35. Jorgensen P, Nelson B, Robinson MD, Chen Y, Andrews B, Tyers M, et al. High-resolution genetic mapping with ordered arrays of *Saccharomyces cerevisiae* deletion mutants. *Genetics*. 2002; 162: 1091–9. PMID: 12454058
36. Kaerberlein M, Andalis AA, Liszt GB, Fink GR, Guarente L. *Saccharomyces cerevisiae* SSD1-V confers longevity by a Sir2p-independent mechanism. *Genetics*. 2004; 166: 1661–72. PMID: 15126388
37. Stettler S, Chiannilkulchai N, Hermann-Le Denmat S, Lalo D, Lacroute F, Sentenac A, et al. A general suppressor of RNA polymerase I, II and III mutations in *Saccharomyces cerevisiae*. *Mol Gen Genet*. 1993; 239: 169–76. <https://doi.org/10.1007/bf00281615> PMID: 8510644

38. Wheeler RT, Kupiec M, Magnelli P, Abeijon C, Fink GR. A *Saccharomyces cerevisiae* mutant with increased virulence. *Proc Natl Acad Sci U S A*. 2003; 100: 2766–70. <https://doi.org/10.1073/pnas.0437995100> PMID: 12589024
39. Li L, Lu Y, Qin LX, Bar-Joseph Z, Werner-Washburne M, Breeden LL. Budding yeast *SSD1-V* regulates transcript levels of many longevity genes and extends chronological life span in purified quiescent cells. *Mol Biol Cell*. 2009; 20: 3851–64. <https://doi.org/10.1091/mbc.E09-04-0347> PMID: 19570907
40. Björk GR, Huang B, Persson OP, Byström AS. A conserved modified wobble nucleoside (mcm5s2U) in lysyl-tRNA is required for viability in yeast. *RNA*. 2007; 13: 1245–55. <https://doi.org/10.1261/ma.558707> PMID: 17592039
41. Klassen R, Grunewald P, Thuring KL, Eichler C, Helm M, Schaffrath R. Loss of anticodon wobble uridine modifications affects tRNA(Lys) function and protein levels in *Saccharomyces cerevisiae*. *PLoS One*. 2015; 10: e0119261. <https://doi.org/10.1371/journal.pone.0119261> PMID: 25747122
42. Jablonowski D, Frohloff F, Fichtner L, Stark MJ, Schaffrath R. *Kluyveromyces lactis* zymocin mode of action is linked to RNA polymerase II function via Elongator. *Mol Microbiol*. 2001; 42: 1095–105. <https://doi.org/10.1046/j.1365-2958.2001.02705.x> PMID: 11737649
43. Huang B, Lu J, Byström AS. A genome-wide screen identifies genes required for formation of the wobble nucleoside 5-methoxycarbonylmethyl-2-thiouridine in *Saccharomyces cerevisiae*. *RNA*. 2008; 14: 2183–94. <https://doi.org/10.1261/ma.1184108> PMID: 18755837
44. Ralser M, Kuhl H, Ralser M, Werber M, Lehrach H, Breitenbach M, et al. The *Saccharomyces cerevisiae* W303-K6001 cross-platform genome sequence: insights into ancestry and physiology of a laboratory mutt. *Open Biol*. 2012; 2: 120093. <https://doi.org/10.1098/rsob.120093> PMID: 22977733
45. Matheson K, Parsons L, Gammie A. Whole-Genome Sequence and Variant Analysis of W303, a Widely-Used Strain of *Saccharomyces cerevisiae*. *G3 (Bethesda)*. 2017; 7: 2219–26. <https://doi.org/10.1534/g3.117.040022> PMID: 28584079
46. Costigan C, Gehrung S, Snyder M. A synthetic lethal screen identifies SLK1, a novel protein kinase homolog implicated in yeast cell morphogenesis and cell growth. *Mol Cell Biol*. 1992; 12: 1162–78. <https://doi.org/10.1128/mcb.12.3.1162> PMID: 1545797
47. Lee KS, Irie K, Gotoh Y, Watanabe Y, Araki H, Nishida E, et al. A yeast mitogen-activated protein kinase homolog (Mpk1p) mediates signalling by protein kinase C. *Mol Cell Biol*. 1993; 13: 3067–75. <https://doi.org/10.1128/mcb.13.5.3067> PMID: 8386319
48. Mazzoni C, Zarzov P, Rambourg A, Mann C. The SlT2 (Mpk1) map kinase homolog is involved in polarized cell growth in *Saccharomyces cerevisiae*. *J Cell Biol*. 1993; 123: 1821–33. <https://doi.org/10.1083/jcb.123.6.1821> PMID: 8276900
49. Martin H, Castellanos MC, Cenamor R, Sanchez M, Molina M, Nombela C. Molecular and functional characterization of a mutant allele of the mitogen-activated protein-kinase gene *SLT2(MPK1)* rescued from yeast autolytic mutants. *Curr Genet*. 1996; 29: 516–22. PMID: 8662190
50. Ibeas JI, Yun DJ, Damsz B, Narasimhan ML, Uesono Y, Ribas JC, et al. Resistance to the plant PR-5 protein osmotin in the model fungus *Saccharomyces cerevisiae* is mediated by the regulatory effects of *SSD1* on cell wall composition. *Plant J*. 2001; 25: 271–80. PMID: 11208019
51. Belcourt MF, Farabaugh PJ. Ribosomal frameshifting in the yeast retrotransposon Ty: tRNAs induce slippage on a 7 nucleotide minimal site. *Cell*. 1990; 62: 339–52. [https://doi.org/10.1016/0092-8674\(90\)90371-k](https://doi.org/10.1016/0092-8674(90)90371-k) PMID: 2164889
52. Tukenmez H, Xu H, Esberg A, Byström AS. The role of wobble uridine modifications in +1 translational frameshifting in eukaryotes. *Nucleic Acids Res*. 2015; 43: 9489–99. <https://doi.org/10.1093/nar/gkv832> PMID: 26283182
53. Otero G, Fellows J, Li Y, de Bizemont T, Dirac AM, Gustafsson CM, et al. Elongator, a multisubunit component of a novel RNA polymerase II holoenzyme for transcriptional elongation. *Mol Cell*. 1999; 3: 109–18. PMID: 10024884
54. Raisner RM, Madhani HD. Genomewide screen for negative regulators of sirtuin activity in *Saccharomyces cerevisiae* reveals 40 loci and links to metabolism. *Genetics*. 2008; 179: 1933–44. <https://doi.org/10.1534/genetics.108.088443> PMID: 18689887
55. Noma A, Sakaguchi Y, Suzuki T. Mechanistic characterization of the sulfur-relay system for eukaryotic 2-thiouridine biogenesis at tRNA wobble positions. *Nucleic Acids Res*. 2009; 37: 1335–52. <https://doi.org/10.1093/nar/gkn1023> PMID: 19151091
56. Leidel S, Pedrioli PG, Bucher T, Brost R, Costanzo M, Schmidt A, et al. Ubiquitin-related modifier Urm1 acts as a sulphur carrier in thiolation of eukaryotic transfer RNA. *Nature*. 2009; 458: 228–32. <https://doi.org/10.1038/nature07643> PMID: 19145231

57. Nakai Y, Nakai M, Hayashi H. Thio-modification of yeast cytosolic tRNA requires a ubiquitin-related system that resembles bacterial sulfur transfer systems. *J Biol Chem.* 2008; 283: 27469–76. <https://doi.org/10.1074/jbc.M804043200> PMID: 18664566
58. Mir SS, Fiedler D, Cashikar AG. Ssd1 is required for thermotolerance and Hsp104-mediated protein disaggregation in *Saccharomyces cerevisiae*. *Mol Cell Biol.* 2009; 29: 187–200. <https://doi.org/10.1128/MCB.02271-07> PMID: 18936161
59. Koplin A, Preissler S, Ilina Y, Koch M, Scior A, Erhardt M, et al. A dual function for chaperones SSB-RAC and the NAC nascent polypeptide-associated complex on ribosomes. *J Cell Biol.* 2010; 189: 57–68. <https://doi.org/10.1083/jcb.200910074> PMID: 20368618
60. Kammenga JE. The background puzzle: how identical mutations in the same gene lead to different disease symptoms. *FEBS J.* 2017; 284: 3362–73. <https://doi.org/10.1111/febs.14080> PMID: 28390082
61. Hou J, van Leeuwen J, Andrews BJ, Boone C. Genetic Network Complexity Shapes Background-Dependent Phenotypic Expression. *Trends Genet.* 2018; 34: 578–86. <https://doi.org/10.1016/j.tig.2018.05.006> PMID: 29903533
62. Rezgui VA, Tyagi K, Ranjan N, Konevega AL, Mittelstaet J, Rodnina MV, et al. tRNA tKUUU, tQUUG, and tEUUC wobble position modifications fine-tune protein translation by promoting ribosome A-site binding. *Proc Natl Acad Sci U S A.* 2013; 110: 12289–94. <https://doi.org/10.1073/pnas.1300781110> PMID: 23836657
63. Bauer F, Matsuyama A, Candiracci J, Dieu M, Scheliga J, Wolf DA, et al. Translational control of cell division by Elongator. *Cell Rep.* 2012; 1: 424–33. <https://doi.org/10.1016/j.celrep.2012.04.001> PMID: 22768388
64. Fernandez-Vazquez J, Vargas-Perez I, Sanso M, Buhne K, Carmona M, Paulo E, et al. Modification of tRNA(Lys) UUU by elongator is essential for efficient translation of stress mRNAs. *PLoS Genet.* 2013; 9: e1003647. <https://doi.org/10.1371/journal.pgen.1003647> PMID: 23874237
65. Amberg DC, Burke DJ, Strathern JN. *Methods in Yeast Genetics.* Cold Spring Harbor, N Y: Cold Spring Harbor Laboratory Press; 2005.
66. Johansson MJO. Determining if an mRNA is a Substrate of Nonsense-Mediated mRNA Decay in *Saccharomyces cerevisiae*. In: Wajapeyee N, Gupta R, editors. *Eukaryotic Transcriptional and Post-Transcriptional Gene Expression Regulation.* Methods Mol Biol. 1507. New York, NY: Humana Press; 2017. pp. 169–77.
67. Brachmann CB, Davies A, Cost GJ, Caputo E, Li J, Hieter P, et al. Designer deletion strains derived from *Saccharomyces cerevisiae* S288C: a useful set of strains and plasmids for PCR-mediated gene disruption and other applications. *Yeast.* 1998; 14: 115–32.
68. Sikorski RS, Hieter P. A system of shuttle vectors and yeast host strains designed for efficient manipulation of DNA in *Saccharomyces cerevisiae*. *Genetics.* 1989; 122: 19–27. PMID: 2659436
69. Fiorentini P, Huang KN, Tishkoff DX, Kolodner RD, Symington LS. Exonuclease I of *Saccharomyces cerevisiae* functions in mitotic recombination in vivo and in vitro. *Mol Cell Biol.* 1997; 17: 2764–73. <https://doi.org/10.1128/mcb.17.5.2764> PMID: 9111347
70. Christianson TW, Sikorski RS, Dante M, Shero JH, Hieter P. Multifunctional yeast high-copy-number shuttle vectors. *Gene.* 1992; 110: 119–22. [https://doi.org/10.1016/0378-1119\(92\)90454-w](https://doi.org/10.1016/0378-1119(92)90454-w) PMID: 1544568
71. Gehrke CW, Kuo KC. Ribonucleoside Analysis by Reversed-Phase High Performance Liquid Chromatography. In: Gehrke CW, Kuo KC, editors. *Journal of Chromatography Library. Chromatography and Modification of Nucleosides Analytical Methods for Major and Modified Nucleosides: HPLC, GC, MS, NMR, UV and FT-IR.* Amsterdam: Elsevier; 1990. pp. A3–A71.
72. Xu F, Zhou Y, Byström AS, Johansson MJO. Identification of factors that promote biogenesis of tRNACGA(Ser). *RNA Biol.* 2018; 15: 1286–94. <https://doi.org/10.1080/15476286.2018.1526539> PMID: 30269676
73. Edmondson DG, Smith MM, Roth SY. Repression domain of the yeast global repressor Tup1 interacts directly with histones H3 and H4. *Genes Dev.* 1996; 10: 1247–59. <https://doi.org/10.1101/gad.10.10.1247> PMID: 8675011
74. Lu J, Huang B, Esberg A, Johansson MJO, Byström AS. The *Kluyveromyces lactis* gamma-toxin targets tRNA anticodons. *RNA.* 2005; 11: 1648–54. <https://doi.org/10.1261/ma.2172105> PMID: 16244131